

**PAPER**

Quantum simulation of bosons with the contracted quantum eigensolver

OPEN ACCESS**RECEIVED**

10 July 2023

REVISED

3 September 2023

ACCEPTED FOR PUBLICATION



14 September 2023

PUBLISHED

5 October 2023

Original Content from
this work may be used
under the terms of the
[Creative Commons
Attribution 4.0 licence](#).

Any further distribution
of this work must
maintain attribution to
the author(s) and the title
of the work, journal
citation and DOI.

Yuchen Wang¹ , LeeAnn M Sager-Smith²  and David A Mazziotti^{1,*} ¹ Department of Chemistry and The James Franck Institute, The University of Chicago, Chicago, IL 60637, United States of America² Department of Chemistry and physics, Saint Mary's College, Notre Dame, IN 46556, United States of America

* Author to whom any correspondence should be addressed.

E-mail: damaz@uchicago.edu**Keywords:** bosons, quantum computing, vibrational motion, correlation, simulation**Abstract**

Quantum computers are promising tools for simulating many-body quantum systems due to their potential scaling advantage over classical computers. While significant effort has been expended on many-fermion systems, here we simulate a model entangled many-boson system with the contracted quantum eigensolver (CQE). We generalize the CQE to many-boson systems by encoding the bosonic wavefunction on qubits. The CQE provides a compact ansatz for the bosonic wave function whose gradient is proportional to the residual of a contracted Schrödinger equation. We apply the CQE to a bosonic system, where N quantum harmonic oscillators are coupled through a pairwise quadratic repulsion. The model is relevant to the study of coupled vibrations in molecular systems on quantum devices. Results demonstrate the potential efficiency of the CQE in simulating bosonic processes such as molecular vibrations with good accuracy and convergence even in the presence of noise.

1. Introduction

Quantum computers have the potential to surpass classical computers in simulating quantum many-body systems [1–6]. There has been tremendous effort to develop simulation algorithms for noisy intermediate-scale quantum (NISQ) devices [7–19]. Among them, the simulation of fermions is specifically interesting because electrons are fermions and hence, their simulation is directly related to molecular behavior. In this paper, however, we focus on many-boson systems [20–27] that are equally important in nature.

Computing the quantum energies of bosons is a fundamental problem in quantum mechanics, and it has various applications in different domains. Applications include the study of atoms and molecules [28], condensed-matter systems such as superfluids, superconductors, and Bose–Einstein condensates [29–34], light and other optical phenomena [35, 36], chemical reactions [37], and quantum devices [38]. In principle, the simulation of bosons should be more straightforward than fermions since they do not require the additional encoding to account for fermion antisymmetry. However, since qubits are hard-core bosons, which means they cannot occupy the same orbital, simulation of bosons is not exactly the same as simulating qubit particles. Here we employ a straightforward encoding that represents each bosonic orbital with N qubits where N is the number of bosons, which leads to linear scaling in both N and the number of qubits.

The extension to bosonic systems in this work is achieved with the contracted quantum eigensolver (CQE) [39]. CQE is a general algorithm for solving the many-body Schrödinger equation on a quantum computer. It is inspired from the contracted Schrödinger equation (CSE), which projects the Schrödinger equation onto a two-particle basis [40–44]. The key challenge in solving the CSE is to ensure the N -representability, that the two-electron reduced density matrix (2-RDM) must represent an N -particle wavefunction, which can be achieved on a classical computer with approximation techniques such as the cumulant expansion [45, 46] or on a quantum computer with tomographic measurements [39, 47–52]. The method has been applied to calculate ground- and excited-state energies and properties with accurate

results [53, 54]. Comparing to popular methods such as the variational quantum eigensolver (VQE), the CQE uses a verifiably exact ansatz, which is expected to converge to an exact solution in a noiseless environment [50]. Moreover, we use the gradient equation derived from the CSE to guide the optimization, avoiding searches that can become extremely costly in high-dimensional parameter spaces.

In this paper, we apply the CQE to a system that consists of multiple one-dimensional harmonic oscillators. Given that the harmonic oscillator provides the fundamental model for quantum vibrations, we can consider the system where N quantum harmonic oscillators are coupled by a pairwise potential as a basic approximation to coupled molecular vibrational modes [55–61]. The elegance of this system resides in the fact that an analytical solution can be obtained through a normal coordinate transformation and can thus be directly used to benchmark the performance of CQE on noiseless simulators as well as on NISQ devices. Using this prototype, the energies are computed with CQE and benchmarked with exact solutions.

2. Theory

We review the quantum algorithm for solving the anti-Hermitian part of the CSE (ACSE) in section 2.1 and introduce the bosonic mapping used in this work in section 2.2. The coupled harmonic oscillator system is presented in section 2.3.

2.1. Anti-Hermitian CSE

Consider a quantum system of N identical bosons in r orbitals described by the Schrödinger equation

$$\hat{H}|\Psi\rangle = E|\Psi\rangle. \quad (1)$$

Here E and $|\Psi\rangle$ are the many-boson ground-state energy and wave function, and \hat{H} is the Hamiltonian operator. One can write the Hamiltonian in second-quantized form as

$$\hat{H} = \sum_{pqst} {}^2K_{st}^{pq} \hat{b}_p^\dagger \hat{b}_q^\dagger \hat{b}_t \hat{b}_s \quad (2)$$

in which 2K is the reduced Hamiltonian matrix, the indices ranging from one to r denote the orbitals. The \hat{b}_p^\dagger and \hat{b}_p are the bosonic creation and annihilation operators with respect to the p th orbital. Taking the expectation value of the above equation yields the energy as a function of the two-particle reduced density matrix 2D (2-RDM).

$$E = \sum_{pqst} {}^2K_{st}^{pq} \langle \Psi | \hat{b}_p^\dagger \hat{b}_q^\dagger \hat{b}_t \hat{b}_s | \Psi \rangle = \text{Tr} [{}^2K {}^2D] \quad (3)$$

where

$${}^2D_{st}^{pq} = \langle \Psi | \hat{b}_p^\dagger \hat{b}_q^\dagger \hat{b}_t \hat{b}_s | \Psi \rangle. \quad (4)$$

The ACSE, which has been used to solve for energies and properties of many-particle systems [39, 44, 62, 63], has the following form

$$\langle \Psi | \left[\hat{b}_p^\dagger \hat{b}_q^\dagger \hat{b}_t \hat{b}_s, \hat{H} \right] | \Psi \rangle = 0. \quad (5)$$

The ACSE can be solved for the 2-RDM without direct computation of the many-particle wavefunction, and in previous work we have presented an algorithm to solve the ACSE on quantum devices [39]. The method is briefly reviewed here. Consider the variational ansatz,

$$|\Psi_{n+1}\rangle = e^{\hat{A}_n} |\Psi_n\rangle \quad (6)$$

where \hat{A}_n is a two-body anti-hermitian operator

$$\hat{A}_n = \sum_{pqst} {}^2A_n^{pq:st} \hat{b}_p^\dagger \hat{b}_q^\dagger \hat{b}_t \hat{b}_s, \quad (7)$$

that constructs the unitary transformation for updating the wavefunction. Here we select \hat{A}_n to be the residual of the ACSE

$${}^2A_n^{pq:st} = \langle \Psi_n | \left[\hat{b}_p^\dagger \hat{b}_q^\dagger \hat{b}_t \hat{b}_s, \hat{H} \right] | \Psi_n \rangle. \quad (8)$$

Table 1. ACSE-based CQE algorithm for the quantum simulation of many-boson systems.**Algorithm. ACSE-based CQE method for bosons.**

Given $n = 0$ and $0 < \delta \leq 1$.

Choose initial wave function $|\Psi_0\rangle$.

Repeat until $\|{}^2A_n\|$ is small.

Step 1: prepare $|\Lambda_n^\pm\rangle$ from $|\Lambda_n^\pm\rangle = e^{\pm i\delta\hat{H}}|\Psi_n\rangle$,

Step 2: measure 2A_n from ${}^2A_n^{ijkl} = \frac{1}{2i\delta} \left(\langle \Lambda_n^+ | \hat{b}_i^\dagger \hat{b}_j^\dagger \hat{b}_k \hat{b}_l | \Lambda_n^+ \rangle - \langle \Lambda_n^- | \hat{b}_i^\dagger \hat{b}_j^\dagger \hat{b}_k \hat{b}_l | \Lambda_n^- \rangle \right)$,

Step 3: prepare $|\Psi_{n+1}\rangle$ from $|\Psi_{n+1}\rangle = e^{\epsilon\hat{A}_n}|\Psi_n\rangle$,

Step 4: measure ${}^2D_{n+1}$ from ${}^2D_{n+1}^{pq;st} = \langle \Psi_{n+1} | \hat{b}_p^\dagger \hat{b}_q^\dagger \hat{b}_t \hat{b}_s | \Psi_{n+1} \rangle$,

Step 5: iterate Steps 3 and 4 to minimize the energy with respect to ϵ ,

Step 6: set $n = n + 1$.

From equation (3), we take the derivative of energy at the n th iteration with respect to ${}^2A_n^{pq;st}$ and obtain

$$\frac{\partial E_n}{\partial ({}^2A_n^{pq;st})} = -\epsilon \langle \Psi_n | \left[\hat{b}_p^\dagger \hat{b}_q^\dagger \hat{b}_t \hat{b}_s, \hat{H} \right] | \Psi_n \rangle + O(\epsilon^2), \quad (9)$$

which shows that the negative of the residual of the ACSE yields the derivative of E_n . Following the gradient downhill, we obtain an iterative expression for the 2-RDM

$${}^2D_{n+1}^{pq;st} = {}^2D_n^{pq;st} + \epsilon \langle \Psi_n | \left[\hat{b}_p^\dagger \hat{b}_q^\dagger \hat{b}_t \hat{b}_s, \hat{A}_n \right] | \Psi_n \rangle + O(\epsilon^2), \quad (10)$$

which can be expressed as a linear functional of the 1-, 2-, and 3-RDMs. On a classical computer we can approximately reconstruct the 3-RDM from the lower-order RDMs. On quantum computers we can measure the 2-RDM by measuring the expectation value of tomographic Pauli strings which does not require higher order RDMs [50, 64]. Similarly, we can measure \hat{A}_n in equation (7) from numerical gradient techniques that are in principle exact when the step size is infinitesimal. Table 1 summarizes the ACSE-based CQE algorithm for bosons. The algorithm, which is similar to the algorithm for fermions in [64], is applicable to any bosonic two-body Hamiltonian including the Hamiltonian of coupled harmonic oscillators, discussed in section 2.3. In practical terms, the simulation and numerical gradient outcomes are collectively influenced by the step size, sampling error, and device noises. The effects of these factors will be further discussed in the results section.

2.2. Boson to qubit mapping

Since qubits are hard-core bosons, we require N qubits to encode the wavefunction of N bosons in a single orbital. The total number of qubits required for bosonic system simulation is then equal to the number of bosons times the number of orbitals. We map the creation and annihilation operators onto qubits using the following equations, which is different from the fermionic transformation such as the Jordan–Wigner mapping [65]:

$$b_{j,r}^\dagger = \underbrace{1 \otimes 1 \otimes \dots \otimes 1}_{r \times (j-1) + r - 1} \otimes \left(\frac{X - iY}{2} \right) \otimes 1 \otimes \dots \otimes 1 \quad (11)$$

$$b_{j,r} = \underbrace{1 \otimes 1 \otimes \dots \otimes 1}_{r \times (j-1) + r - 1} \otimes \left(\frac{X + iY}{2} \right) \otimes 1 \otimes \dots \otimes 1 \quad (12)$$

where $b_{j,r}^\dagger$ and $b_{j,r}$ represents annihilate and create the j th boson in the r th orbital. By summing over indices j , we obtain the bosonic annihilation and creation operator in r th orbital

$$b_r^\dagger = \frac{1}{\sqrt{N}} \sum_{j=1}^N b_{r,j}^\dagger, b_r = \frac{1}{\sqrt{N}} \sum_{j=1}^N b_{r,j}. \quad (13)$$

2.3. Hamiltonian of coupled harmonic oscillators

Our model system consists of N spinless bosons subject to harmonic interactions in the one-dimensional space first inspected by Sage [55] and later by other authors [56–61, 66]. The one-body interactions are

attractive with a scaled force constant Z and the pairwise two-body interactions are repulsive. The Hamiltonian can be written as

$$\hat{H} = \sum_{i=1}^N h(i) + \sum_{i>j} u(i,j) = \sum_{i>j} h(i,j) \quad (14)$$

where

$$h(i) = -\frac{\partial^2}{\partial x_i^2} + Zx_i^2, \quad (15)$$

$$u(i,j) = -(x_i - x_j)^2, \quad (16)$$

and

$$h(i,j) = \frac{1}{N-1} [h(i) + h(j)] + u(i,j). \quad (17)$$

Comparing equations (2) and (17), we obtain the matrix elements of the two-particle reduced Hamiltonian (2K)

$${}^2K_{st}^{pq} = \frac{1}{N-1} \left(\delta_s^p \langle q|\hat{h}|t\rangle + \delta_t^q \langle p|\hat{h}|s\rangle \right) + \langle pq|\hat{u}|st\rangle. \quad (18)$$

It has been shown by Sage [55] that, using the following normal coordinate transformation, we can decouple the N harmonic oscillators,

$$Q_i = \begin{cases} \frac{1}{\sqrt{N}} \sum_{i=1}^N x_i, & i = 1 \\ \frac{1}{\sqrt{i(i-1)}} \left[(i-1)x_i - \sum_{i=1}^{N-1} x_i \right], & 2 \leq i \leq N \end{cases} \quad (19)$$

where the Hamiltonian in terms of these coordinates is

$$\hat{H} = \sum_{i=1}^N \left(-\frac{\partial^2}{\partial Q_i^2} \right) + Zx_1^2 + (Z-N) \sum_{i=2}^N x_i^2. \quad (20)$$

The system becomes N uncoupled harmonic oscillators with the first one having a force constant of \sqrt{Z} and the remaining $(N-1)$ indistinguishable ones having force constants of $\sqrt{Z-N}$. The system is analytically solvable and the exact ground-state energy is given as

$$E_{\text{exact}} = \sqrt{Z} + (N-1) \sqrt{Z-N} \quad (21)$$

which can be used to benchmark results from numerical simulations. The n th natural orbital of the system has the form

$$\phi_n = (2^n n! \sqrt{\pi})^{-\frac{1}{2}} \gamma^{\frac{1}{2}} H_n(\gamma x) e^{-\gamma^2 x^2 / 2} \quad (22)$$

where $H_n(\gamma x)$ is the n th order Hermite polynomial and γ is a scaling factor that is determined from diagonalizing the exact 1-RDM of the system. For simulation with CQE as described below, we use the natural-orbital basis because it provides fast convergence, though other bases would also work with larger basis sizes. Note that the analytical solution in principle can be viewed as the full configuration interaction (CI) obtained from an infinite basis set. The numerical solution in a finite basis set is thus be an upper bound to the analytical solution as can be seen from figure 1(a).

To approach the problem from a numerical perspective, first, consider the mean-field approximation in which the energy can be easily written down as

$$E_{\text{MF}} = N\sqrt{Z-N+1}. \quad (23)$$

The value N/Z quantifies the correlation effects. When N/Z approaches zero, the two-body interaction is negligible compared to the one-body term. The system can then be viewed as N almost-independent harmonic oscillators with the mean-field solution approaching the exact solution. When N/Z approaches 1, the correlation effects cannot be ignored and the energy of the mean-field approximation starts to deviate

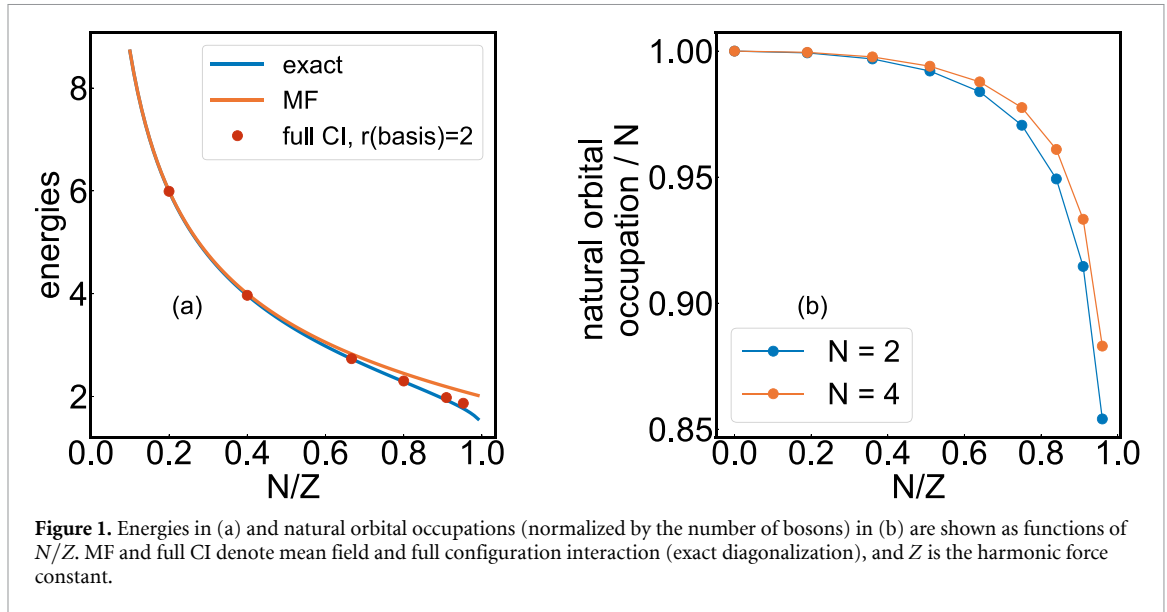


Figure 1. Energies in (a) and natural orbital occupations (normalized by the number of bosons) in (b) are shown as functions of N/Z . MF and full CI denote mean field and full configuration interaction (exact diagonalization), and Z is the harmonic force constant.

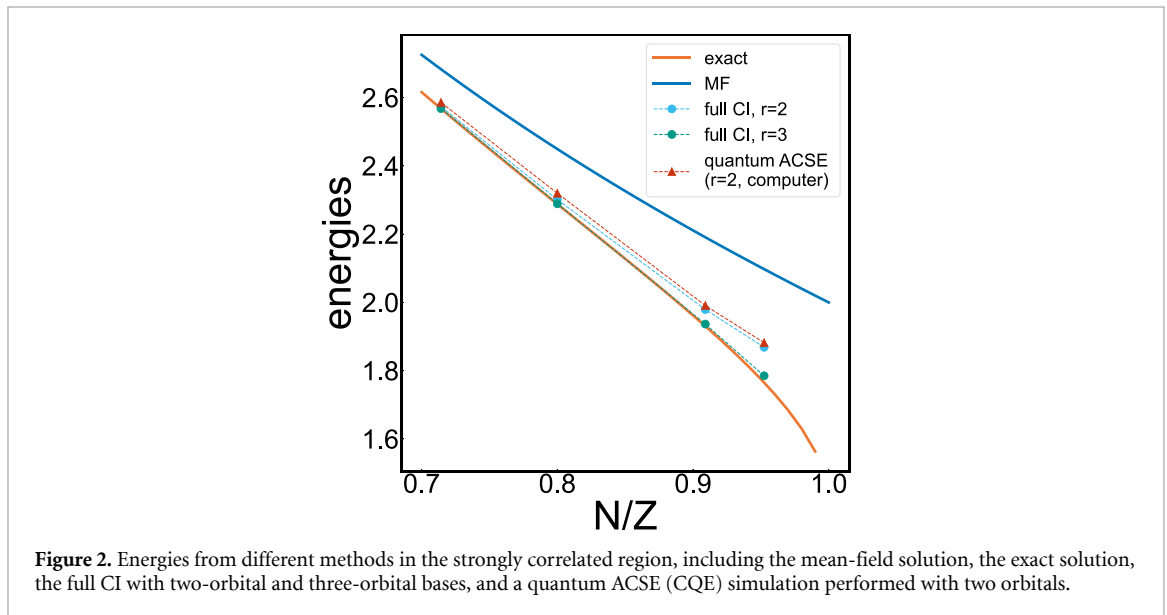


Figure 2. Energies from different methods in the strongly correlated region, including the mean-field solution, the exact solution, the full CI with two-orbital and three-orbital bases, and a quantum ACSE (CQE) simulation performed with two orbitals.

from the full CI result as shown in figure 1(a). This can also be seen from figure 1(b), where the occupation number of the first natural orbital is plotted as a function of N/Z . The normalized value starts from 1, where all bosons are in the lowest orbitals, and drops significantly when N/Z is close to 1, which is a result of strong correlation of the bosons. It is also worth noting that when more bosons are present, the correlation effect is reduced. This can be conceptualized as the mean-field approximation being improved by the environment that the $(N - 1)$ bosons form when N becomes large and eventually infinite.

For capturing the correlation effects correctly, different numerical methods have been proposed besides full CI, including the connected moments expansion (CMX) methods [58] and the reduced Hamiltonian interpolation (RHI) [60, 61]. Discussion of these classical methods is beyond the scope of the article and is not pursued here. In this paper, we will implement CQE in strong correlated regime and benchmark with full CI and analytical exact results.

3. Applications

3.1. Model Hamiltonian simulations

We perform simulations on a quantum state-vector simulator and IBMQ Lagos devices. 8192 shots were used for experiments on devices. For the stepsize to evaluate $A_n^{pq;st}$, we used 0.01 for simulator and 0.5 for quantum devices. The convergence tolerance for the simulator is set to 10^{-7} . All experiments were conducted with the Qiskit package [67].

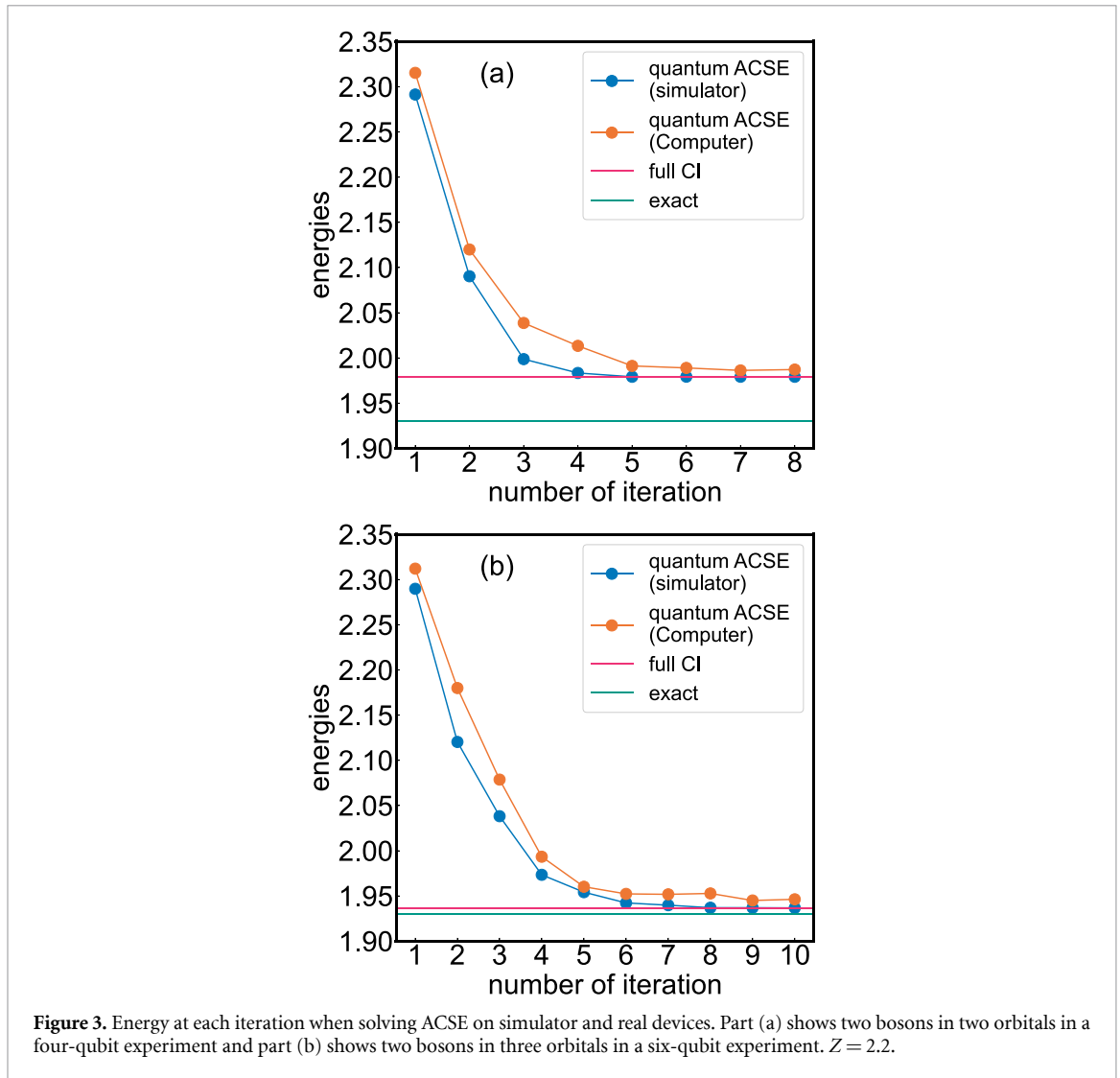


Figure 3. Energy at each iteration when solving ACSE on simulator and real devices. Part (a) shows two bosons in two orbitals in a four-qubit experiment and part (b) shows two bosons in three orbitals in a six-qubit experiment. $Z = 2.2$.

We first compare the energies from different methods in the strong correlated region ($N/Z > 0.7$, $N = 2$, $r = 2$) in figure 2. The highest and lowest curves correspond to the mean-field and exact solutions, respectively. It is clear that the mean-field solution fails in the strongly correlated region. We also plot the full CI results with basis-set sizes $r = 2, 3$ for benchmarking purposes. As can be seen, CI with a three-orbital basis is sufficient to capture most of the correlation energy. The two-orbital basis performs almost as well as the three-orbital basis when $N/Z < 0.8$ but deteriorates afterwards. This basis-set truncation error exists for finite basis sets and can be improved easily with larger basis sets. The curve with triangle tickmarks shows the CQE results performed on actual quantum computers. We observe that the difference between CQE and full CI with the same basis set is much smaller than the error caused by basis-size truncation, which indicates that the accuracy of CQE is limited by the basis-set size and we expect the CQE to achieve greater accuracy with larger basis sets.

3.2. Convergence of quantum ACSE

In figure 3(a) we show a convergence diagram with two bosons in two orbitals, where a total number of four qubits are used to represent the wavefunction of the system. The starting guess places both bosons in the lowest orbital, which is the ground state in the absence of correlation. It can be seen that for both the quantum simulator and the quantum computer, the optimization converges to a stable solution in eight or fewer iterations. On an ideal state-vector simulator the error arises from the non-infinitesimal stepsize employed when evaluating \hat{A}_n as well as the first-order Trotter error. Despite such error, the CQE achieves an accuracy within 10^{-7} comparing to full CI, verifying the exactness of the CQE algorithm [39]. In the presence of device noise and sampling error, the results on a real quantum computer are only ~ 0.01 higher than those on the noise-free simulator. This error is also fairly uniform across the iterations of the optimization.

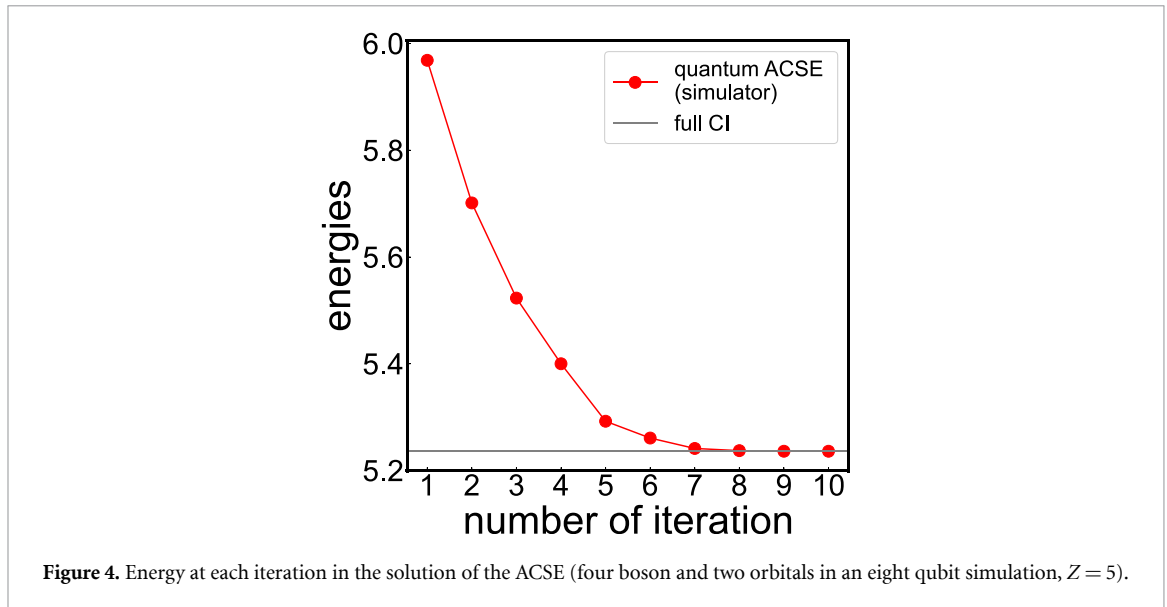


Figure 4. Energy at each iteration in the solution of the ACSE (four boson and two orbitals in an eight qubit simulation, $Z = 5$).

Table 2. Full CI and CQE(computer) energies of the ground- and first-excited states for the coupled harmonic oscillator system ($N = 2$, $r = 2$). For ground and excited ACSE calculations, starting guesses of $|0101\rangle$ and $|1001\rangle$ are used respectively.

N/Z	Ground		Excited	
	Exact	CQE	Exact	CQE
0.2	5.990 719	5.998 725	11.665 688	11.672 398
0.4	3.968 379	3.972 838	7.492 909	7.498 718
0.8	2.367 377	2.370 212	4.221 183	4.231 868

Second, we study the effect of basis-set size by including an additional basis function. In figure 3(a), the CQE results are close to those from the full CI with two orbitals, but are relatively different from those from the calculation in the infinite-orbital basis set. By increasing the basis-set size by one, we observe in figure 3(b) that our CQE result is much closer to the exact result with a difference of 0.015. This demonstrates that the error in figure 3(a) comes mostly from the finite basis set and that the CQE can reproduce a low error relative to full CI with larger basis-set sizes.

Third, we perform a simulation with four bosons in two orbitals on the quantum simulator. This calculation shows that the algorithm can be straightforwardly extended to more bosons on noise-free simulators while still preserving good accuracy. The convergence diagram is plotted in figure 4. As can be seen, the CQE still offers a near-exact solution on ideal simulators in approximately ten iterations. For molecules with more vibrational degrees of freedom, a linearly increasing number of qubits should fulfill the task, which is advantageous over certain classical algorithms.

Lastly, we explore the ability of CQE in calculating excited states. Noted that in the derivation of the ACSE in section IIA, we do not explicitly require the energy to be the ground-state energy. Indeed, the system of differential equations in equations (9) and (10) is capable of producing energy and 2-RDM solutions of the ACSE for both ground and excited states [68]. Even though excited states correspond to local stationary points rather than global energy minima of the optimization, they can be obtained from a reasonable starting guess, usually at the level of a Hartree–Fock calculation. In table 2, we report the ground- and first excited-state energies, obtained from full CI and CQE on quantum devices. It can be seen that performance of CQE is quite uniform in both ground- and excited-state optimization, giving an error less than 0.01 for every selected point (except for the excited state at $N/Z = 0.8$). Here we show the CQE can be extended to treat excited states, and in future work we will show that excited states and ground state can be treated on an equal footing [69, 70] on quantum devices.

4. Conclusions

The simulation of bosonic systems is a fundamental problem in quantum mechanics with applications ranging from atomic and molecular physics, condensed-matter physics, and particle physics to quantum optics, quantum chemistry, and quantum computing. We generalize the CQE to simulate many-boson systems without losing generality in treating strong correlation. In particular, we simulate a molecular

vibrational problem by solving the ACSE of the system with CQE. The many-boson wavefunction is encoded to qubits by grouping N qubits to represent a single bosonic orbital, where N is the number of bosons in the system. The total number of required qubits thus scales linearly with the number of both bosons and orbitals. Despite the simplicity of the encoding, the algorithm makes use of a 2-RDM-like tomography with complexity up to $O(r^4)$ where r is the number of qubits, demonstrating a potential polynomial scaling advantage over classical methods.

We apply CQE to a system of vibrationally coupled quantum harmonic oscillators. Quantum harmonic oscillators—each of which is a good approximation to a single molecular vibration—are coupled by a pairwise potential to account for the coupled vibrational modes. This model can be used to treat coupled molecular modes when a normal-mode separation could be costly. We report simulation results on both a quantum simulator and a quantum device. On a noise-free simulator, the CQE results are almost exact, where the only errors arise from the Trotterized unitary transformation and the small but not infinitesimal stepsize taken in measuring the residual of ACSE. On NISQ devices, we achieve a very good accuracy in comparison with full CI results for both ground and excited states. The present work provides an important step towards the simulation of molecular vibrations on quantum devices. Future work will extend the present formalism to treat mixed fermion and boson systems. Given that the CSE ansatz is verifiably exact, we anticipate such systems can also be accurately treated on quantum computers with tools like the CQE.

Data availability statement

All data that support the findings of this study are included within the article (and any supplementary files).

Acknowledgments

D A M gratefully acknowledges the Department of Energy, Office of Basic Energy Sciences, Grant DE-SC0019215 and the U.S. National Science Foundation Grant Nos. CHE-2155082, CHE-2035876, and DMR-2037783 and IBMQ. The views expressed are of the authors and do not reflect the official policy or position of IBM or the IBM Q team.

ORCID iDs

Yuchen Wang  <https://orcid.org/0000-0003-0479-3776>

LeeAnn M Sager-Smith  <https://orcid.org/0000-0001-6760-9134>

David A Mazziotti  <https://orcid.org/0000-0002-9938-3886>

References

- [1] Feynman R 1982 Simulating physics with computers *Int. J. Theor. Phys.* **21** 467
- [2] Lloyd S 1996 Universal quantum simulators *Science* **273** 1073
- [3] Abrams D S and Lloyd S 1997 Simulation of many-body Fermi systems on a universal quantum computer *Phys. Rev. Lett.* **79** 2586
- [4] Aspuru-Guzik A, Dutoi A D, Love P J and Head-Gordon M 2005 Simulated quantum computation of molecular energies *Science* **309** 1704
- [5] Lanyon B P et al 2010 Towards quantum chemistry on a quantum computer *Nat. Chem.* **2** 106
- [6] McArdle S, Endo S, Aspuru-Guzik A, Benjamin S C and Yuan X 2020 Quantum computational chemistry *Rev. Mod. Phys.* **92** 015003
- [7] Kitaev A Y 1995 Quantum measurements and the abelian stabilizer problem (arXiv:quant-ph/9511026)
- [8] Abrams D S and Lloyd S 1999 Quantum algorithm providing exponential speed increase for finding eigenvalues and eigenvectors *Phys. Rev. Lett.* **83** 5162
- [9] Dobšiček M, Johansson G, Shumeiko V and Wendin G 2007 Arbitrary accuracy iterative quantum phase estimation algorithm using a single ancillary qubit: a two-qubit benchmark *Phys. Rev. A* **76** 030306
- [10] Paesani S, Gentile A A, Santagati R, Wang J, Wiebe N, Tew D P, O'Brien J L and Thompson M G 2017 Experimental Bayesian quantum phase estimation on a silicon photonic chip *Phys. Rev. Lett.* **118** 100503
- [11] Peruzzo A, McClean J, Shadbolt P, Yung M-H, Zhou X-Q, Love P J, Aspuru-Guzik A and O'Brien J L 2014 A variational eigenvalue solver on a photonic quantum processor *Nat. Commun.* **5** 4213
- [12] Wecker D, Hastings M B and Troyer M 2015 Progress towards practical quantum variational algorithms *Phys. Rev. A* **92** 042303
- [13] McClean J R, Romero J, Babbush R and Aspuru-Guzik A 2016 The theory of variational hybrid quantum-classical algorithms *New J. Phys.* **18** 023023
- [14] Kandala A, Mezzacapo A, Temme K, Takita M, Brink M, Chow J M and Gambetta J M 2017 Hardware-efficient variational quantum eigensolver for small molecules and quantum magnets *Nature* **549** 242
- [15] Wang D, Higgott O and Brierley S 2019 Accelerated variational quantum eigensolver *Phys. Rev. Lett.* **122** 140504
- [16] Tang H L, Shkolnikov V, Barron G S, Grimsley H R, Mayhall N J, Barnes E and Economou S E 2021 Qubit-adapt-vqe: an adaptive algorithm for constructing hardware-efficient ansätze on a quantum processor *PRX Quantum* **2** 020310
- [17] Higgott O, Wang D and Brierley S 2019 Variational quantum computation of excited states *Quantum* **3** 156
- [18] Grimsley H R, Economou S E, Barnes E and Mayhall N J 2019 An adaptive variational algorithm for exact molecular simulations on a quantum computer *Nat. Commun.* **10** 3007

- [19] Fedorov D A, Peng B, Govind N and Alexeev Y 2022 VQE method: a short survey and recent developments *Mater. Theory* **6** 1
- [20] Huh J, Guerreschi G G, Peropadre B, McClean J R and Aspuru-Guzik A 2015 Boson sampling for molecular vibronic spectra *Nat. Photon.* **9** 615
- [21] Wang C S *et al* 2020 Efficient multiphoton sampling of molecular vibronic spectra on a superconducting bosonic processor *Phys. Rev. X* **10** 021060
- [22] Ollitrault P J, Baiardi A, Reiher M and Tavernelli I 2020 Hardware efficient quantum algorithms for vibrational structure calculations *Chem. Sci.* **11** 6842
- [23] Lötstedt E, Yamanouchi K, Tsuchiya T and Tachikawa Y 2021 Calculation of vibrational eigenenergies on a quantum computer: application to the Fermi resonance in CO₂ *Phys. Rev. A* **103** 062609
- [24] Wang Y, Mulvihill E, Hu Z, Lyu N, Shivpuje S, Liu Y, Soley M B, Geva E, Batista V S and Kais S 2023 Simulating open quantum system dynamics on NISQ computers with generalized quantum master equations *J. Chem. Theory Comput.* **19** 4851
- [25] Kovyshin A, Skogh M, Broo A, Mensa S, Sahin E, Crain J and Tavernelli I 2023 A quantum computing implementation of nuclearelectronic orbital (NEO) theory: toward an exact pre-Born-Oppenheimer formulation of molecular quantum systems *J. Chem. Phys.* **158** 214119
- [26] Benavides-Riveros C L, Wolff J, Marques M A L and Schilling C 2020 Reduced density matrix functional theory for bosons *Phys. Rev. Lett.* **124** 180603
- [27] Schmidt J, Fadel M and Benavides-Riveros C L 2021 Machine learning universal bosonic functionals *Phys. Rev. Res.* **3** L032063
- [28] Alon O E, Streltsov A I and Cederbaum L S 2008 Multiconfigurational time-dependent hartree method for bosons: many-body dynamics of bosonic systems *Phys. Rev. A* **77** 033613
- [29] Zhang Z, Chen L, Yao K-X and Chin C 2021 Transition from an atomic to a molecular Bose-Einstein condensate *Nature* **592** 708
- [30] Liu X, Li J I A, Watanabe K, Taniguchi T, Hone J, Halperin B I, Kim P and Dean C R 2022 Crossover between strongly coupled and weakly coupled exciton superfluids *Science* **375** 205
- [31] Hartke T, Oreg B, Turnbaugh C, Jia N and Zwierlein M 2023 Direct observation of nonlocal fermion pairing in an attractive Fermi-Hubbard gas *Science* **381** 82
- [32] Kasprzak J *et al* 2006 Bose-Einstein condensation of exciton polaritons *Nature* **443** 409
- [33] Byrnes T, Kim N Y and Yamamoto Y 2014 Exciton-polariton condensates *Nat. Phys.* **10** 803
- [34] Safaei S and Mazziotti D A 2018 Quantum signature of exciton condensation *Phys. Rev. B* **98** 045122
- [35] Mitchell M W, Lundeen J S and Steinberg A M 2003 Super-resolving phase measurements with a multiphoton entangled state *Nature* **429** 161
- [36] Balili R, Hartwell V, Snoke D, Pfeiffer L and West K 2007 Bose-Einstein condensation of microcavity polaritons in a trap *Science* **316** 1007
- [37] Lin R, Mognini P, Papariello L, Tsatsos M C, Lévêque C, Weiner S E, Fasshauer E, Chitra R and Lode A U 2020 MCTDH-X: the multiconfigurational time-dependent hartree method for indistinguishable particles software *Quantum Sci. Technol.* **5** 024004
- [38] Devoret M H and Schoelkopf R J 2013 Superconducting circuits for quantum information: an outlook *Science* **339** 1169
- [39] Smart S E and Mazziotti D A 2021 Quantum solver of contracted eigenvalue equations for scalable molecular simulations on quantum computing devices *Phys. Rev. Lett.* **126** 070504
- [40] Nakatsuji H and Yasuda K 1996 Direct determination of the quantum-mechanical density matrix using the density equation *Phys. Rev. Lett.* **76** 1039
- [41] Mazziotti D A 1998 Contracted Schrödinger equation: determining quantum energies and two-particle density matrices without wave functions *Phys. Rev. A* **57** 4219
- [42] Mukherjee D and Kutzelnigg W 2001 Irreducible Brillouin conditions and contracted Schrödinger equations for n-electron systems. I. The equations satisfied by the density cumulants *J. Chem. Phys.* **114** 2047
- [43] Alcoba D R and Valdemoro C 2001 Family of modified-contracted Schrödinger equations *Phys. Rev. A* **64** 062105
- [44] Mazziotti D A 2006 Anti-hermitian contracted Schrödinger equation: direct determination of the two-electron reduced density matrices of many-electron molecules *Phys. Rev. Lett.* **97** 143002
- [45] Mazziotti D A 1999 Pursuit of N-representability for the contracted Schrödinger equation through density-matrix reconstruction *Phys. Rev. A* **60** 3618
- [46] Mazziotti D A 2000 Complete reconstruction of reduced density matrices *Chem. Phys. Lett.* **326** 212
- [47] Mazziotti D A, Smart S E and Mazziotti A R 2021 Quantum simulation of molecules without fermionic encoding of the wave function *New J. Phys.* **23** 113037
- [48] Boyn J-N, Lykhin A O, Smart S E, Gagliardi L and Mazziotti D A 2021 Quantum-classical hybrid algorithm for the simulation of all-electron correlation *J. Chem. Phys.* **155** 244106
- [49] Smart S E and Mazziotti D A 2022 Accelerated convergence of contracted quantum eigensolvers through a quasi-second-order, locally parameterized optimization *J. Chem. Theory Comput.* **18** 5286
- [50] Smart S E and Mazziotti D A 2023 Verifiably exact solution of the electronic Schrödinger equation on quantum devices (arXiv:2303.00758)
- [51] Smart S E and Mazziotti D A 2022 Many-fermion simulation from the contracted quantum eigensolver without fermionic encoding of the wave function *Phys. Rev. A* **105** 062424
- [52] Smart S E, Boyn J-N and Mazziotti D A 2022 Resolving correlated states of benzene with an error-mitigated contracted quantum eigensolver *Phys. Rev. A* **105** 022405
- [53] Snyder J W Jr and Mazziotti D A 2011 Photoexcited conversion of gauche-1, 3-butadiene to bicyclobutane via a conical intersection: energies and reduced density matrices from the anti-hermitian contracted Schrödinger equation *J. Chem. Phys.* **135** 024107
- [54] Boyn J-N and Mazziotti D A 2021 Accurate singlet-triplet gaps in biradicals via the spin averaged anti-hermitian contracted Schrödinger equation *J. Chem. Phys.* **154** 134103
- [55] Sage M L 1970 Orbitals and geminals for particles moving in a harmonic potential *Theor. Chim. Acta* **19** 179
- [56] Pruski S, Maćkowiak J and Missuno O 1972 Reduced density matrices of a system of N coupled oscillators 3. The eigenstructure of the p-particle matrix for the ground-state *Rep. Math. Phys.* **3** 241
- [57] Cohen L and Lee C 1985 Exact reduced density matrices for a model problem *J. Chem. Phys.* **26** 3105
- [58] Cioslowski J 1987 Connected moments expansion: a new tool for quantum many-body theory *Phys. Rev. Lett.* **58** 83
- [59] Mancini J D, Fessatidis V and Bowen S P 1999 Moments expansions for the correlation energy of an exactly solvable problem *Phys. Lett. A* **259** 280
- [60] Mazziotti D A and Herschbach D R 1999 Boson correlation energies from reduced Hamiltonian interpolation *Phys. Rev. Lett.* **83** 5185

- [61] Mazziotti D A and Herschbach D R 2000 Boson correlation energies and density matrices from reduced Hamiltonian interpolation *Phys. Rev. A* **62** 043603
- [62] Mazziotti D A 2007 Multireference many-electron correlation energies from two-electron reduced density matrices computed by solving the anti-Hermitian contracted Schrödinger equation *Phys. Rev. A* **76** 1
- [63] Gidofalvi G and Mazziotti D A 2007 Multireference self-consistent-field energies without the many-electron wave function through a variational low-rank two-electron reduced-density-matrix method *J. Chem. Phys.* **127** 244105
- [64] Smart S E and Mazziotti D A 2021 Lowering tomography costs in quantum simulation with a symmetry projected operator basis *Phys. Rev. A* **103** 012420
- [65] Jordan P and Wigner E 1928 Über das paulische äquivalenzverbot *Eur. Phys. J. A* **47** 631–51
- [66] Gidofalvi G and Mazziotti D A 2004 Boson correlation energies via variational minimization with the two-particle reduced density matrix: exact N-representability conditions for harmonic interactions *Phys. Rev. A* **69** 042511
- [67] Qiskit Contributors 2023 Qiskit: an open-source framework for quantum computing (<https://doi.org/10.5281/zenodo.2573505>)
- [68] Wang Y and Mazziotti D A 2023 Electronic excited states from a variance-based contracted quantum eigensolver (arXiv:2305.03044 [quant-ph])
- [69] Yarkony D R, Xie C, Zhu X, Wang Y, Malbon C L and Guo H 2019 Diabatic and adiabatic representations: electronic structure caveats *Comput. Theor. Chem.* **1152** 41
- [70] Wang Y, Guan Y, Guo H and Yarkony D R 2021 Enabling complete multichannel nonadiabatic dynamics: a global representation of the two-channel coupled, 1 , 2^1A and 1^3A states of NH_3 using neural networks *J. Chem. Phys.* **154** 094121